Medical Journal of Ahl al-Bayt University, Vol.3, No.1, Aug.2024

Effect of Topically Applied Sodium Fusidate Loaded-Silver Nanoparticles as Gel Dosage Form on Burn-Induced Model in Rats

Omar Saleh Abdulkader [1], Abdulkareem Hameed Abd[2], Ahmed Najim Abood [3]

omar.saleh@basra-college.edu.iq
nkh00@nahrainuniv.edu.iq
ahmed.abood@uobasrah.edu.iq

[1]Department of Pharmacology, Basrah University College of Science and Technology, Basra, Iraq
[2]Department of Pharmacology, College of Medicine, Al-Nahrain University, Baghdad, Iraq
[3]Department of Pharmaceutics, College of Pharmacy, University of Basra, Basra, Iraq

ABSTRACT

Aim: Creating and analyzing a new formulation of sodium fusidate loaded-silver nanoparticles in the form of a gel. Procedure: sodium fusidate loaded-silver nanoparticles prepared by chemical reduction method using trisodium citrate as the reducing agent to produce silver nanoparticles firstly. Then the gel prepared by using carbomer 940 and triethanolamine. sodium fusidate loaded-silver nanoparticles was characterized by globular diameter, polydispersity index (PDI) and pH. Results: The novel formula had (668.2±0.2nm) globular diameter, normal homogeneous dispersion (PDI, 0.567±0.002) and pH (6.2±0.05). Conclusions: To our knowledge, this is the first sodium fusidate loaded-silver nanoparticles nano-drug delivery system. It has promising pre-clinical and clinical uses.

Keywords: Sodium Fusidate, Silver Nanoparticles, Gel, Topical,

INTRODUCTION

Burn injuries are a frequently overlooked form of trauma that have the potential to impact individuals of all backgrounds, at any given moment and in any location. Burn injuries can result from various sources such as heat, cold, radiation, chemical exposure (Jeschke *et al.*, 2020).

Severe burns, irrespective of their etiology, result in a profoundly chaotic inflammatory reaction in the body shortly after the injury (Longo and Greenhalgh, 2019).

Raised levels of chemokines, cytokines, and acute phase proteins, and a state of enhanced metabolism are characteristic of the inflammatory and stress responses. This condition arises from a persistent sympathetic activity that can persist beyond the initial stage of treatment (Rowan *et al.*, 2015). Following an injury, the burn wound can be classified into three distinct zones: the coagulation zone (where the central portion is most severely damaged), the stasis or ischemia zone

(marked by reduced blood flow that can potentially be saved), and the hyperemia zone (the outer area of the wound defined by increased inflammation and blood vessel dilation) (Osuka *et al.*, 2014).

In addition to cytokines and other inflammatory mediators, stress hormones such as catecholamines and cortisones are released at the site of damage. These substances have effects throughout the body. Burn injury typically leads to distributive shock (Rae *et al.*, 2016).

After a burn injury, the hypermetabolic state can last up to 36 months beyond the original insult (Jeschke *et al.*, 2011). This state includes elevated basal metabolic rate, heightened body temperature, overall loss of body protein, degradation of muscle tissue, and enhanced production of acute-phase proteins (for instance, insulin-like growth factor 1 (IGF-1), which promotes tissue growth). These effects lead to the breakdown of organs, and ultimately death (Figure 2) (Sidossis *et al.*, 2015).

Patients who have had severe burns are more likely to acquire infectious problems. Patients with severe burn burns frequently develop ventilator-associated pneumonia. (Lachiewicz *et al.*, 2017). Patients can acquire additional sources of infection from their own microbiota, which is related with their skin, respiratory tract, and intestines. The compromised immune system increases their vulnerability to infection, primarily from bacteria but also from yeast, fungi, and viruses. This also enhances the virulence of specific pathogens, leading to the development of multiple organ failure, affecting the liver, lungs, kidneys and heart. (Rech *et al.*, 2019).

The primary objective of wound treatment is to mitigate the risk of severe infection, expedite the healing process, and minimize scarring and suffering experienced by patients. Various treatments are available for wound management, primarily involving debridement, autografts, and the application of therapeutic agents. These approaches play an increasingly crucial role in the management of complex wounds (Na and Wei, 2021).

The management of burn wound infections and the process of skin regeneration are intricate and have been the subject of extensive research for many years. The emergence of antibiotic-resistant microbes has been linked to increased resistance to topical antimicrobial medicines in burn injuries, posing a significant hazard to public health. Therefore, it is imperative to create novel antimicrobial agents with even greater potential.

Nanotechnology has brought to the utilization of particles composed of diverse materials, yet its shared characteristic is their size range of 10–1000 nm (Malekzad *et al.*, 2018).

Nanomedicine has the potential to enhance therapy for infected burns and promote superior skin recovery. Nanotechnology has demonstrated remarkable antibacterial efficacy against drug-resistant germs and can help expedite the regeneration of skin damaged by burns (Zhu *et al.*, 2014).

Platforms with silver at the nanoscale, such as silver nanoparticles AgNPs, and hydrogels containing silver, have been used in the treatment of burn wounds. AgNPs were utilized as an antibacterial substance for the treatment of skin wounds. They demonstrated a significant antimicrobial activity and the potential to be employed in wound dressings (Konop *et al.*, 2016).

Silver offers a significantly expansive surface area for bacterial interaction. The nanoparticles adhere to the cell membrane and infiltrate the bacterium (Rai *et al.*, 2009). Bacterial membranes comprise proteins containing sulfur, and AgNPs interact with these proteins as well as with DNA, so impeding their function (Matsumura *et al.*, 2003).

Sodium fusidate is a sodium salt derivative of fusidic acid, which is a bacteriostatic steroid antibiotic. It is commonly applied topically in the form of creams, ointments, and eyedrops. However, it can also be administered orally as tablets or through injections. It originated from the fungus *Fusidium coccineum*. Additionally, it has been extracted from *Mucor ramannianus* and *Isaria kogana* (Falagas *et al.*, 2008).

Sodium fusidate functions as a bacteriostatic agent by impeding the removal of elongation factor G (EF-G) from the ribosome, hence inhibiting bacterial protein production(Leclercq *et al.*, 2000). It forms a bond with EF-G upon translocation and the breakdown of GTP (guanosine-5'-triphosphate) (Bodley *et al.*, 1969).

This contact hinders the essential conformational changes required for the release of EF-G from the ribosome, hence impeding the process of protein synthesis.

Sodium fusidate exhibits activity against *Staphylococcus aureus*, most *coagulase-positive staphylococci*, *Beta-hemolytic streptococci*, *Corynebacterium species*, and the majority of *clostridium species*. It lacks effective action against *enterococci* or the majority of Gram-negative bacteria, with the exception of *Moraxella, Neisseria, Legionella pneumophila,* and *Bacteroides fragilis* (O'Neill and Chopra, 2004).

Sodium fusidate, when applied topically, is utilized as a remedy for acne vulgaris. Sodium fusidate is commonly used as a treatment for acne, however its effectiveness in reducing acne symptoms is frequently limited (Spelman, 1999). Sodium fusidate may be a viable therapy option for people suffering from chronic osteomyelitis associated to prosthetic joints(Wolfe, 2011).

In this study, we utilized sodium fusidate and AgNPs to create a gel dosage form. To the best of our knowledge, this is the first report on the impact of topically applied sodium fusidate loaded-silver nanoparticles in gel form on an animal model with burn injuries.

Methods

Formulation of sodium fusidate loaded-silver nanoparticles gel

The chemical reduction method was employed to synthesize silver nanoparticles using trisodium citrate (TSC) as the reducing agent. Trisodium citrate reduces Ag+ ions, resulting in the formation of metallic silver (Ag0), which subsequently agglomerates into oligomeric clusters. These clusters ultimately form metallic colloidal silver particles. (Wiley *et al.*, 2005).

Sliver nitrate (AgNO3) and trisodium citrate were used as starting materials for preparation of silver nanoparticles. All solutions of reacting materials were prepared in distilled water. A 50 ml of 0.001 M AgNO3 was heated to boil. To this solution 5 ml. of 1% trisodium citrate was added drop by drop. Throughout the procedure, the solutions were forcefully mixed and heated until a

noticeable change in color, specifically a pale-yellow, occurred. Subsequently, the substance has been removed from the heating apparatus and agitated until it reached ambient temperature. (Vashishth and Kaushik, 2017).

A 10 ml of sodium fusidate 2% solution was added to 10 ml of silver nanoparticles solution (previously prepared) to produce a diluted 20 ml solution of sodium fusidate 1% loaded-silver nanoparticles.

A 0.5% (0.1g) of carbomer 940 was added to 20 ml of drug loaded-silver nanoparticles solution. the mixture was stirred by mechanical stirrer until homogeneous dispersion occur then drops of 98% triethanolamine (TEA) were added to this dispersion till get viscous or thick appearance gel (Islam *et al.*, 2004).

Formulation of silver nanoparticles gel

A 50 ml solution containing 0.001 M AgNO3 was heated until it reached its boiling point. To this solution, 5 ml of a 1% trisodium citrate has been added gradually, drop by drop. Throughout the procedure, the solutions were forcefully mixed and heated till a noticeable change in color occurred, specifically a pale-yellow color. Subsequently, the substance was removed from the heating apparatus and stirred until it reached the room temperature.
(Vashishth and Kaushik, 2017).

A 0.5% (0.1g) of carbomer 940 was added to 20 ml of silver nanoparticles solution. the mixture was stirred by mechanical stirrer until homogeneous dispersion occur then drops of 98% triethanolamine (TEA) were added to this dispersion till get viscous or thick appearance gel (Islam *et al.*, 2004).

Formulation of sodium fusidate gel

A 0.5% (0.1g) of carbomer 940 was added to 20 ml of sodium fusidate 1% solution. the mixture was stirred by mechanical stirrer until homogeneous dispersion occur then drops of 98% triethanolamine (TEA) were added to this dispersion till get viscous or thick appearance gel (Islam *et al.*, 2004).

Evaluation of the Sodium fusidate Loaded Silver Nanoparticles

Particle Size and Polydispersity Index Analysis

The particle size and polydispersity index (PDI) of Sodium fusidate Loaded Silver Nanoparticles were determined by photon correlation spectroscopy using Zetasizer NanoZS, which analyses fluctuation in light scattering based on Brownian particle motions and light scatter (Eid *et al.*, 2019).

The particle size analysis was conducted at a temperature of 25°C using an angle of detection of 173°(Sanad *et al.*, 2010). The diameter and polydispersity index of Sodium fusidate Loaded Silver Nanoparticles were obtained directly from the device. All samples were measured in triplicates.

Measurement of pH

The pH readings of the samples were determined using a pH meter. Prior to each usage, the pH meter was calibrated using a buffer solution with a pH value of 4, 7, and 9. The samples were analyzed directly on the electrode. The formulation's pH was measured in triplicate at 25ºC, and mean values were calculated (Rubenick *et al.*, 2017).

***In vivo* Animal Laboratory Work**

Experimental Animals

Thirty adult male rats (between 8 and 12 weeks of age; and body weight 200- 300g at arrival) were used in this study. All the animals were provided unrestricted access to water and food with standard pellets. The animals were kept in plastic cages within a room that was temperature-controlled at standard temperature and humidity conditions and a 12-hr light/dark cycle throughout the study, per the guide for care and use of laboratory animal (Albus, 2012).

Rats were assigned randomly into five experimental groups, each containing 6 rats; all of them were sacrificed at the end of the study (after 14 days). Blood samples were collected, and the skin tissue of the wound was isolated for histological and immunohistochemistry (IHC) analysis (Cheng *et al.*, 2018).

With details of treatment, groups of the animal list as followings (application of treatments were done twice daily on burns):

Group I (C): Apparently healthy (non-burned, untreated) rats

Group II (B): Burned untreated rats

Group III (SF): Burned rats treated with topical sodium fusidate 1% gel

Group IV (AgNPs): Burned rats treated with topical silver nanoparticles gel

Group V (SF AgNPs): Burned rats and treated with a topical sodium fusidate 1% loaded -silver nanoparticles gel

Blood Parameters Assay

Fresh blood samples were collected via cardiac puncture by using 5ml disposable syringe in an EDTA-glass tube (Hoff, 2000). Blood samples were collected from all animals in the study groups one day after burning wound induction, as well as at the day 7 and at the end of the experiment, to estimate white blood cell count (WBC), neutrophils and monocytes.

Burn Model

All experimental animals were anesthetized by injection of ketamine (100mg/kg) and xylazine (20mg/kg) (Frank and Kämpfer, 2003) . A gap of 10-15 minutes was left for anesthesia; their dorsal surface hair was shaved with an electric clipper. The dorsal skin surface of all rats was decontaminated by cleaning it with sterile saline, followed by disinfection using a 10% povidone-iodine solution and 70% ethanol alcohol. The burns were developed by applying a cylindrical stainless-steel rod with a diameter of 1cm that had been heated in boiling water at a temperature

of around 100º C. The rod was maintained in the water for 15 minutes while a thermometer was present to monitor the temperature.

This rod placed on the shaving area of the rat's dorsum for about 45 seconds to produce a third degree burn (Loo *et al.*, 2014). Burns were rinsed immediately with normal saline and left undressed for treatment preparation (Khalil *et al.*, 2016).

Finally, each rat was individually housed in a plastic cage to prevent biting and fighting with other rats and to preserve skin burn treatment. The various prepared treatments were applied to the wound twice daily with follow-up.

Measurement of Burning Area

Wound diameter in mm was measured for each rat at day 0 (promptly after wounding), 7, and 14 post-operations; wound diameter was gauged utilizing an electronic vernier caliper. Simultaneously, the wounds were documented through photography, including measures of their diameter. Throughout the process, the animals were partially sedated using an ether.

Skin Wound Biopsies

On day 14 post-operation, the tissue biopsies of wounds were taken under general anesthesia (ketamine + xylazine) using sterilized scissors and forceps according to the previously mentioned procedure (DiPietro and BURNS, 2003). About 2mm of the directly adjacent skin was included, representing the wound margin tissue after burning the dorsal skin surface. The specimens were fixed in 10% formalin and sent for histological analysis.

Results

Particle Size and Polydispersity Index Analysis for Sodium Fusidate Loaded Silver Nanoparticles

The particle size and polydispersity index (PDI) of sodium fusidate loaded silver nanoparticles were examined by Zetasizer. Findings showed that the formula was regarded within the nano-size range. the formula had a typical uniform dispersion (PDI; 0.567±0.002) and globular diameter (668.2±0.2nm).

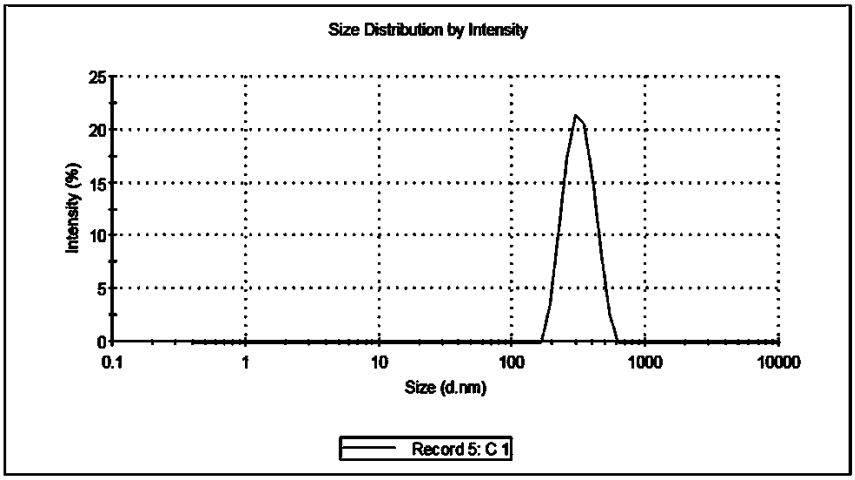

Figure: Globular Diameter (nm) of sodium fusidate loaded silver nanoparticle

Sodium Fusidate Loaded Silver Nanoparticles pH

The sodium fusidate loaded silver nanoparticles was analyzed directly on the probe of the pH meter. The mean value of the final formula pH is (6.2±0.05), making it suitable for topical skin application.

Effect of Sodium Fusidate (SF) gel, Silver Nanoparticles (AgNPs) gel and Sodium Fusidate Loaded Silver Nanoparticles (SF AgNPs) gel on Total and differential WBC of burned laboratory rats

The results of table (2) indicated that the highest significant difference (P≤0.05) was recorded in the leucocytes, Neutrophils and monocytes traits for the period (1st day) and for all treated groups, while the control group recorded the least significant difference (P≤0.05) in the leucocytes, Neutrophils and monocytes traits

As for the period (7th day), the results indicated that the (burned only) group recorded the highest significant difference (P≤0.05) in the leucocytes, Neutrophils and monocytes traits, followed by both (Burned treated with sodium fusidate gel) and (Burned treated with silver nanoparticles gel) groups. While (Burned treated with sodium fusidate loaded silver nanoparticles gel) and the control groups recorded the least significant difference (P≤0.05) in leucocytes, Neutrophils and monocytes traits.

In the period (14th day), the results showed that the (burned only) group recorded the highest significant difference (P≤0.05) in the leucocytes, Neutrophils and monocytes traits, while the (Burned treated with sodium fusidate loaded silver nanoparticles gel) and control group recorded the lowest Significant difference (P≤0.05) in leucocytes, Neutrophils and monocytes traits. Whereas the results did not record any significant difference in the rest of the traits and for all groups and periods.

Table 3-2: Effect of Sf, AgNP and combination on Total and differential WBC of burned male laboratory rats (Mean ± SEM)

Parameter /WBC (10^3/µL)	Control (Without Burn)			Burn Only			Burn treated with SF			Burn treated with Ag NPs			Burn treated with SF Ag NPs		
	1st day	7th day	14th day	1st day	7th day	14th day	1st day	7th day	14th day	1st day	7th day	14th day	1st day	7th day	14th day
Leukocytes	4.90 ± 0.35**c**	4.72 ± 0.33**c**	4.50 ± 0.33**c**	8.93 ± 1.83**a**	8.67 ± 1.77**a**	8.30 ± 1.71**a**	8.92 ± 1.82 **Aa**	8.35 ± 1.39 **Bb**	4.59 ± 0.32 **Cc**	8.92 ± 1.82 **Aa**	8.59 ± 1.75 **Bb**	4.60 ± 0.33 **Cc**	8.90 ± 1.81 **Aa**	4.70 ± 0.33 **Bc**	4.50 ± 0.33 **Bc**
Neutrophils	0.09 ± 0.09**c**	0.08 ± 0.08**c**	0.07 ± 0.07**c**	0.79 ± 0.66**a**	0.77 ± 0.64**a**	0.75 ± 0.63**a**	0.78 ± 0.65 **Aa**	0.74 ± 0.03 **Aa**	0.11 ± 0.11 **Bb**	0.78 ± 0.65 **Aa**	0.73 ± 0.02 **Aa**	0.09 ± 0,09 **Bb**	0.78 ± 0.65 **Aa**	0.08 ± 0.08 **Bc**	0.07 ± 0.07 **Bc**
Lymphocytes	4.85 ± 0.44	4.37 ± 0.39	4.00 ± 0.37	4.08 ± 0.52	4.06 ± 0.51	4.02 ± 0.52	6.00 ± 1.16	5.08 ± 0.99	5.07 ± 0.98	6.83 ± 0.71	6.67 ± 0.69	6.20 ± 0.65	6.80 ± 1.30	6.64 ± 1.26	6.41 ± 1.23
Monocytes	0.07 ± 0.05**b**	0.06 ± 0.04**b**	0.04 ± 0.03**b**	0.21 ± 0.21**a**	0.21 ± 0.27**a**	0.20 ± 0.26**a**	0.21 ± 0.21 **Aa**	0.18 ± 0.22 **Aa**	0.07 ± 0.05 **Bb**	0.20 ± 0.2 **Aa**	0.17 ± 0.00 **Aa**	0.05 ± 0.03 **Bb**	0.20 ± 0.2 **Aa**	0.05 ± 0.03 **Bb**	0.04 ± 0.03 **Bb**
Eosinophil's	0.05 ± 0.05	0.04 ± 0.04	0.02 ± 0.02	0.03 ± 0.03	0.03 ± 0.03	0.02 ± 0.02	0.06 ± 0.06	0.04 ± 0.04	0.03 ± 0.03	0.04 ± 0.00	0.02 ± 0.00	0.03 ± 0.00	0.06 ± 0.00	0.05 ± 0.00	0.04 ± 0.00
Basophils	0.06 ± 0.04	0.05 ± 0.03	0.03 ± 0.02	0.05 ± 0.06	0.04 ± 0.04	0.03 ± 0.04	0.04 ± 0.04	0.03 ± 0.03	0.02 ± 0.02	0.03 ± 0.03	0.03 ± 0.03	0.02 ± 0.02	0.03 ± 0.00	0.03 ± 0.00	0.02 ± 0.00

Capital letters represent significant difference among periods of the same group at P≤0.05level. small letter referred to significant difference among the groups in the same period at P≤0.05 WBC, white blood cell, LSD, least significant difference * P≤0.05 compared to the corresponding control. The values are the mean ± SEM of N=6 rats/group.

Morphological Wound Healing

Effect of Sodium Fusidate (SF) gel, Silver Nanoparticles (AgNPs) gel and Sodium Fusidate Loaded Silver Nanoparticles (SF AgNPs) gel on wound size of burned laboratory rats

As illustrated in Table (3) that indicated the second period, which recorded the significant difference in the rate of wound closure in the all-treated groups compared to burned only group, while the highest significant difference was recorded in the (Burned treated with sodium fusidate loaded silver nanoparticles gel) group. Moreover, the third period showed significant difference in the rate of wound closure in the all-treated groups compared to burned only group, while the highest significant difference was recorded in the (Burned treated with sodium fusidate loaded silver nanoparticles gel) group.

Table 3-3: Effect of SF, AgNps and combination drugs on wound size for three periods of burned laboratory rats

Group	First Period	Second Period	Third Period
	The size of the wound (mm) (first day)	The size of the wound (mm) after 7 days	The size of the wound (mm) after 14 days
Control (without Burn)	No wound	No wound	No wound
Burned Only	13.52± 0.08	12.47± 0.07	7.50± 0.04
Burned treated with sodium fusidate gel	13.47± 0.07	[a] 11.52± 0.05	[a] 3.70± 0.01
Burned treated with sodium silver nanoparticles gel	13.44± 0.07	[b] 10.40± 0.05	[b]3.14± 0.01
Burned treated with sodium fusidate loaded silver nanoparticles gel	13.34± 0.06	[c] 9.60± 0.04	[c] 1.15± 0.01
LSD	N.S	0.05	0.33

small letter referred to significant difference among the groups in the same period at P≤0.05. N.S = non-significant

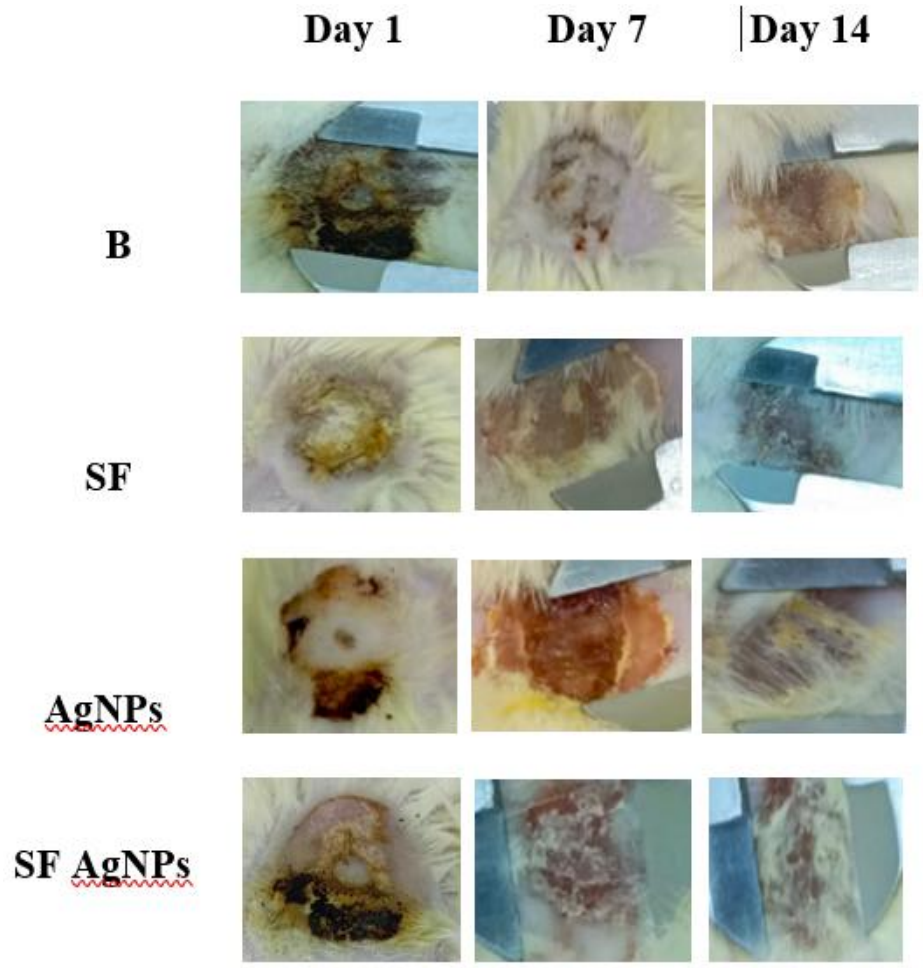

Figure 11: Morphological Representations of Burned Rats Treatment Groups on Different Days. B: Burned Only, SF: Sodium Fusidate Gel, AgNPs : Silver Nanoparticles Gel, SF AgNPs : Sodium Fusidate Loaded Silver Nanoparticles Gel

Wound Histopathological Analysis

Histopathological investigation of the biopsies taken from skin tissue of the burn area was undertaken to provide more evidence on the effects of sodium fusidate loaded silver nanoparticles gel treatment group on rat's skin wounds compared to the healthy, gel-treated group and mupirocin-treated groups. As mentioned in chapter two, the histological serial sections of burn tissues were obtained after sacrificing the animals on post-wounding day 14 and subjected to Hematoxylin and Eosin staining (H&E). The histopathological findings were quantitatively scored f. The following slide images show major skin histopathological changes in all treated groups

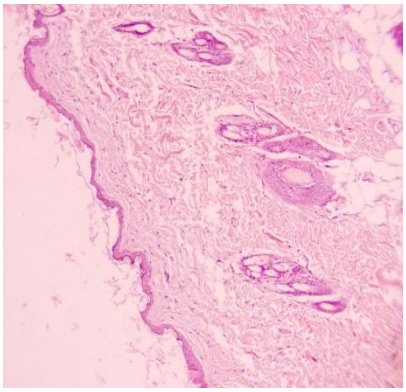

Figure normal structure of skin epidermis and dermis. That show squamous epithelial cell, sebaceous gland, sweat gland and hair follicles. Hematoxylin-eosin X100 (Control healthy group)

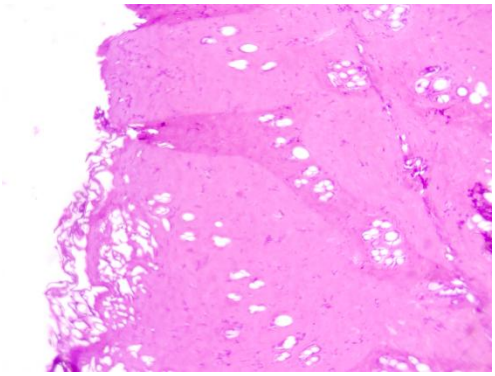

Figure shows necrosis in dermis and epidermis through disappear of cellular and architectures details (structure) and shows vacuoles instead of sebaceous gland and sweat gland and hair follicle. Hematoxylin-eosin X100 (Burned only group)

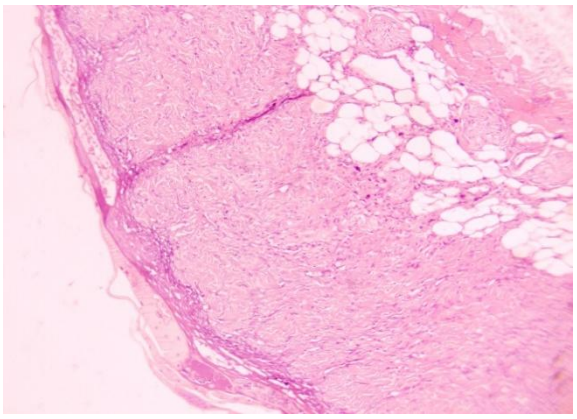

Figure began of healing in skin and epithelization and appeared massive proliferation of collagen also there was filtration in inflammatory cells referred to incomplete healing. Hematoxylin-eosin stain X 100 (Burned treated with sodium fusidate group)

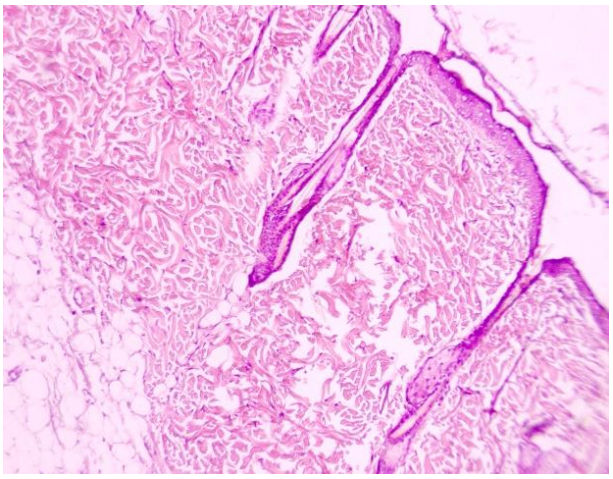

Figure healing in skin and epithelization of epidermis cell and reformed of sebaceous gland and hair follicles in limited number. Also appeared massive proliferation of collagen and filtration in inflammatory cells. Hematoxylin-eosin stain X 100 (Burned treated with silver nanoparticles group)

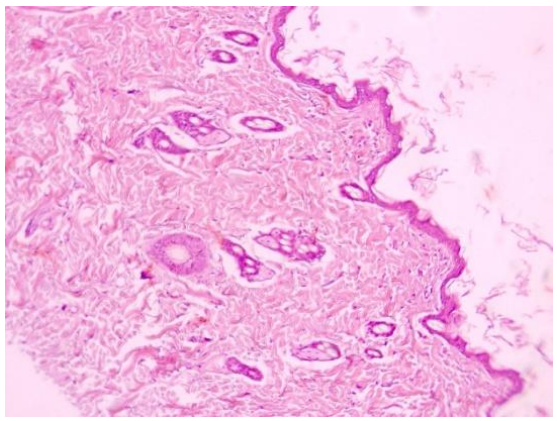

Figure complete repair of skin, with normal epithelial cell. Sebaceous and sweat glands and hair follicles. Reduced bundles of collagen and complete tissue health. Hematoxylin-Eosin stain. X100 (Burned treated with sodium fusidate loaded silver nanoparticles group)

DISCUSSION

Burn injury is a multifaceted traumatic occurrence that has both local and systemic effects, impacting multiple organ systems in addition to the skin. Burn injuries exhibit significant variability in terms of the specific tissues impacted, the degree of severity, and the resulting problems. Damage to nerves can cause substantial injury to muscle, bone, blood vessels, dermal, and epidermal layers of tissue, resulting in subsequent pain (Church *et al.*, 2006).

The primary objective of wound treatment strategies should be to optimize the antibacterial efficacy of topically administered formulations, while concurrently lowering the risk of infections, mitigating bacterial resistance, and facilitating tissue regeneration (Mihai *et al.*, 2019).

This necessitates the adoption of novel techniques to either create new antibiotics or boost the efficacy of current antibiotics (Aruguete *et al.*, 2013).

Consequently, numerous research offers a comprehensive analysis of the management of microbial illness and antibiotic resistance. Nanostructured compounds are a strategy being researched to combat certain forms of bacterial resistance. Hence, Nanoparticles have the potential to be an effective solution as they can both directly attack against bacteria and serve as carriers for antibiotics. This allows them to bypass drug-resistant mechanism in bacteria and aid in the transportation of new medications(Baptista *et al.*, 2018).

Preparation of Sodium Fusidate Loaded Silver Nanoparticles Gel

Although sodium fusidate (SF) is used in different bacterial skin infections therapy, it has limitations like drug resistance, poor skin penetration, local irritation, and sub-optimal efficacy. For this reason, several innovative drug delivery techniques have been developed to promote patient compliance, minimize resistance, amplify the delivery of SF, and bypass traditional formulation restrictions. So, various novel SF preparations have been established, such as dressings made of hydrogel, liposomes, nanofibers, nanocapsules and lipid carriers with nanostructured (Williamson *et al.*, 2017).

The most valuable test to distinguish the micro from nanoparticles is determining its globular size, which should be in the nano range (Parveen *et al.*, 2011). Variable particle size may be used for nanoparticle delivery; however, the smaller particle is easier to uptaken by the cell and shows a larger surface area. Consequently, a smaller particle is related to faster drug release (Singh and Lillard Jr, 2009). The resulting nano-sized particle (668.2 ±0.2nm) showed a considerable small particle size less than 1 μm.

Polydispersity (PDI) is a measure of heterogeneity based on the size of nanoparticles. The small PDI value yielded in the formulation (0.567 ±0.002) may lead to better stability.

For successful wound healing, several endogenous and exogenous elements that participate in the regeneration process are required. The pH values are essential elements that can influence wound metabolism. The intact skin usually states an acidic milieu due to the keratinocyte secretions of amino and fatty acids. This acidic pH fluctuates and is usually reported to be around 4–6 (Schneider *et al.*, 2007).

The prepared formula of sodium fusidate loaded silver nanoparticles shows acidic pH (6.2 ±0.05) that complies with topical skin formulation pH conditions. If the pH value of the wound area becomes alkaline, thus its healing process decreases, pathogenic bacteria can colonize, and antibiotic therapy may be altered (Pourali *et al.*, 2018). On the other hand, SF's Antibacterial effectiveness depends on pH. At acidic pH, SF increased antibacterial activity *in vitro*. Thus, the skin's low pH creates an ideal environment for effective treatment (Lemaire *et al.*, 2011).

Burn exacerbated by infection slows wound healing, contributes significantly to global morbidity and mortality rates, and prompts the investigation of new topical antibiotic therapy approaches (Ladhani *et al.*, 2021).

The results revealed that the sodium fusidate loaded silver nanoparticles treated groups showed a rapid wound contraction of 9.6 ±0.04 around day 7 where healing was much faster than that in other groups. Wound contraction was highly distinguishable around day 14 in all treatment groups compare to burned only group. It was found that burn in sodium fusidate loaded silver nanoparticles treated group appeared to be the highest significant wound contraction 1.15 ±0.01 and this observation was not seen in other groups.

Treatment with sodium fusidate loaded silver nanoparticles produced rapid wound healing by forming normal epithelial cells. Porosity and stability of the formula were the primary reasons for the amplified water adsorption present in wound exudate, forming this new layer on the wound surface and the promotion of autolytic debridement of the wound infection (Zahedi *et al.*, 2010).

Sodium fusidate as a topical antimicrobial has been indicated to have wound-healing effects. Many studies demonstrated that it has a favorable effect on the rate of wound contraction, period of epithelization, and collagen content of wounds in rats (Zhang *et al.*, 2010). However, this was mainly due to its antibacterial role against wound-associated bacteria. Also, it may promote wound closure by enhancing keratinocyte proliferation (Jin *et al.*, 2016). all these are consistent with the results of this study.

As expected, the burned animals group showed a minimal wound closure area rate because no treatment was applied to their wounds. So, the delay in closure compared to other groups depends on the body defense mechanism.

The SF-treated and AgNPs-treated groups also showed a significant wound contraction compared to the burned animal's group around 7 and 14 days.

Inflammation was observed in all treated groups in various degrees as a normal body response post burn (Hamed *et al.*, 2011). However, sodium fusidate loaded silver nanoparticles significantly decreases inflammatory cell infiltration.

Activated neutrophils recruited at the wound site as a response to bacterial degradation product and platelets degranulation provide an inflammatory response (Gurtner *et al.*, 2008). Early neutrophils depletion on day 7 was a good indicator of accelerated wound closure in SF, AgNPs and SF AgNPs treated groups, they especially returned to normal levels on day 14.

Re-epithelialization in burned only group was much slower than in all-treated rats on days 7 and 14. The results demonstrated that the wound of all-treated groups except burned only group had a good level of collagen deposition on day 7. But on day 14, the sodium

fusidate loaded silver nanoparticles treated group, showed a dramatic improvement in collagen, fibrosis, and angiogenesis.

The final stage of wound healing in sodium fusidate loaded silver nanoparticles treated group showed a highly mature dense collagen fiber. This result is consistent with other studies which stated that wound healing in rats after nanoparticles formulation usage shows an increase in collagen deposition, contracture of collagen lattices, stimulation of fibroblast activity, and acceleration of wound repair (Blecher *et al.*, 2012). SF nanoparticles enhance collagenization and decrease inflammation. Also, SF nanoparticles support cell differentiation, adhesion, and proliferation (Norouzi *et al.*, 2015). Furthermore, SF nanoparticles protect wounds from external environmental contaminants and adsorb wound discharges. Their porous nature allows oxygen to permeate, moisturize, and eliminate metabolic waste (Homaeigohar and Boccaccini, 2020).

Various studies on wound healing approved that many drugs loaded nanoparticles improved re-epithelialization, angiogenesis, granulation tissue formation, synthesis of a compact and denser collagen matrix, and upregulation of IL-6 and VEGF (Chereddy *et al.*, 2014). Moreover, drugs loaded nanoparticles decrease mononuclear inflammatory cell infiltration with healed skin structures close to normal healthy epidermis. Specific types of nanoparticle-loaded polymer promoted fibroblast growth and functional tissue remodeling in a way that agrees with the findings in the current study (Xie *et al.*, 2013) .

Drugs-loaded nanoparticles exhibited anti-inflammatory activity (by improved keratinocyte migration), leading to downregulation of IL-1b and COX-2 expression and reduced neutrophil infiltration, regeneration of new connective tissue fibrils and new collagen (Moreno *et al.*, 2015).

SF nanoparticles possess the permeability and porosity of thin membranes, as revealed by many studies (Mohamad *et al.*, 2014), so the histopathological findings of sodium fusidate loaded silver nanoparticles treated group showed a distinguished penetration of the formula effect deeply to the dermis, where appeared as a distinctive fibrous meshwork.

The particle morphology and size play a crucial role in locally applied nanocarriers' absorption and pharmacokinetic properties. After absorption into the wound bed and subcutaneous tissue penetration, nanoparticles reach the dermis' lower strata and be absorbed by the blood capillaries (Rigo *et al.*, 2013).

Angiogenesis refers to the process of forming new blood vessels and has a critical role in many pathological and physiological processes. Angiogenesis is important for wound healing because new vessels deliver oxygen and nutrients to stimulate the actively proliferating cells. The formation of reactive oxygen species (ROS) pathway activation was thought to be the most likely mechanism of angiogenesis (KumaráNethi *et al.*, 2014).

Re-epithelialization, fibroblast, and collagen fibers levels of wounds in burned only animals are significantly lower than in other treated groups. It indicated that the healing quality and the proliferative phase is delayed in wounds without treatment.

REFERENCES

Albus, U. 2012. Guide for the care and use of laboratory animals (8th edn). SAGE Publications Sage UK: London, England.

Aruguete, D. M., Kim, B., Hochella, M. F., *et al.* 2013. Antimicrobial nanotechnology: its potential for the effective management of microbial drug resistance and implications for research needs in microbial nanotoxicology. *J Environmental Science: Processes Impacts,* 15**,** 93-102.

Baptista, P. V., Mccusker, M. P., Carvalho, A., *et al.* 2018. Nano-strategies to fight multidrug resistant bacteria—"A Battle of the Titans". *J Frontiers in microbiology,* 9**,** 381070.

Blecher, K., Martinez, L. R., Tuckman-Vernon, C., *et al.* 2012. Nitric oxide-releasing nanoparticles accelerate wound healing in NOD-SCID mice. *J Nanomedicine: Nanotechnology, Biology Medicine,* 8**,** 1364-1371.

Bodley, J. W., Zieve, F. J., Lin, L., *et al.* 1969. Formation of the ribosome-G factor-GDP complex in the presence of fusidic acid. *J Biochemical biophysical research communications,* 37**,** 437-443.

Cheng, K.-Y., Lin, Z.-H., Cheng, Y.-P., *et al.* 2018. Wound healing in streptozotocin-induced diabetic rats using atmospheric-pressure argon plasma jet. *J Scientific reports,* 8**,** 12214.

Chereddy, K. K., Her, C.-H., Comune, M., *et al.* 2014. PLGA nanoparticles loaded with host defense peptide LL37 promote wound healing. *J Journal of Controlled Release,* 194**,** 138-147.

Church, D., Elsayed, S., Reid, O., *et al.* 2006. Burn wound infections. *J Clinical microbiology reviews,* 19**,** 403-434.

Dipietro, L. A. & Burns, A. W. H. 2003. Methods and Protocols. *J METHODS IN MOLECULAR MEDICINE , NJ HUMANA PRESS, TOTOWA.*

Eid, A. M., Istateyeh, I., Salhi, N., *et al.* 2019. Antibacterial activity of Fusidic acid and sodium Fusidate nanoparticles incorporated in pine oil Nanoemulgel. *J International Journal of Nanomedicine***,** 9411-9421.

Falagas, M. E., Grammatikos, A. P. & Michalopoulos, A. 2008. Potential of old-generation antibiotics to address current need for new antibiotics. *J Expert review of anti-infective therapy,* 6**,** 593-600.

Frank, S. & Kämpfer, H. 2003. Excisional wound healing: an experimental approach. *J Wound healing: methods protocols***,** 3-15.

Gurtner, G. C., Werner, S., Barrandon, Y., *et al.* 2008. Wound repair and regeneration. *J Nature,* 453**,** 314-321.

Hamed, S., Ullmann, Y., Egozi, D., *et al.* 2011. Fibronectin potentiates topical erythropoietin-induced wound repair in diabetic mice. *J Journal of investigative dermatology,* 131**,** 1365-1374.

Hoff, J. 2000. Features-Technique-Methods of Blood Collection in the Mouse-The author outlines various methods of blood collection from mice. *J Lab animal,* 29**,** 47-54.

Homaeigohar, S. & Boccaccini, A. R. 2020. Antibacterial biohybrid nanofibers for wound dressings. *J Acta biomaterialia,* 107**,** 25-49.

Islam, M. T., Rodríguez-Hornedo, N., Ciotti, S., *et al.* 2004. Fourier transform infrared spectroscopy for the analysis of neutralizer-carbomer and surfactant-carbomer interactions in aqueous, hydroalcoholic, and anhydrous gel formulations. *J The AAPS journal,* 6**,** 61-67.

Jeschke, M. G., Gauglitz, G. G., Kulp, G. A., *et al.* 2011. Long-term persistance of the pathophysiologic response to severe burn injury. *J PloS one,* 6**,** e21245.

Jeschke, M. G., Van Baar, M. E., Choudhry, M. A., *et al.* 2020. Burn injury. *J Nature Reviews Disease Primers,* 6**,** 11.

Jin, S. G., Kim, K. S., Kim, D. W., *et al.* 2016. Development of a novel sodium fusidate-loaded triple polymer hydrogel wound dressing: Mechanical properties and effects on wound repair. *J International journal of pharmaceutics,* 497**,** 114-122.

Khalil, A. M., Abd, A. H. & Hussein, B. F. 2016. The Use of Methanolic extract of Boswellia serrata in Combination with Dextrin and Glycerin for Treatment of Experimentally Induced Thermal Injuries in Rabbits. *J Iraqi Journal of Medical Sciences,* 14.

Konop, M., Damps, T., Misicka, A., *et al.* 2016. Certain aspects of silver and silver nanoparticles in wound care: a minireview. *J Journal of Nanomaterials,* 2016**,** 47-47.

Kumaránethi, S., Kumarábarui, A. & Ranjanápatra, C. 2014. Bioconjugated gold nanoparticles accelerate the growth of new blood vessels through redox signaling. *J Chemical communications,* 50**,** 14367-14370.

Lachiewicz, A. M., Hauck, C. G., Weber, D. J., *et al.* 2017. Bacterial infections after burn injuries: impact of multidrug resistance. *J Clinical Infectious Diseases,* 65**,** 2130-2136.

Ladhani, H. A., Yowler, C. J. & Claridge, J. A. 2021. Burn wound colonization, infection, and sepsis. *J Surgical infections,* 22**,** 44-48.

Leclercq, R., Bismuth, R., Casin, I., *et al.* 2000. In vitro activity of fusidic acid against streptococci isolated from skin and soft tissue infections. *J Journal of Antimicrobial Chemotherapy,* 45**,** 27-29.

Lemaire, S., Van Bambeke, F., Pierard, D., *et al.* 2011. Activity of fusidic acid against extracellular and intracellular Staphylococcus aureus: influence of pH and comparison with linezolid and clindamycin. *J Clinical Infectious Diseases,* 52**,** S493-S503.

Longo, D. & Greenhalgh, D. 2019. Management of burns. *J N. Engl. J. Med.,* 380**,** 2349-2359.

Loo, Y., Wong, Y.-C., Cai, E. Z., *et al.* 2014. Ultrashort peptide nanofibrous hydrogels for the acceleration of healing of burn wounds. *J Biomaterials,* 35**,** 4805-4814.

Malekzad, H., Mirshekari, H., Sahandi Zangabad, P., *et al.* 2018. Plant protein-based hydrophobic fine and ultrafine carrier particles in drug delivery systems. *J Critical reviews in biotechnology,* 38**,** 47-67.

Matsumura, Y., Yoshikata, K., Kunisaki, S.-I., *et al.* 2003. Mode of bactericidal action of silver zeolite and its comparison with that of silver nitrate. *J Applied environmental microbiology,* 69**,** 4278-4281.

Mihai, M. M., Dima, M. B., Dima, B., *et al.* 2019. Nanomaterials for wound healing and infection control. *J Materials Science Engineering: C,* 12**,** 2176.

Mohamad, N., Amin, M. C. I. M., Pandey, M., *et al.* 2014. Bacterial cellulose/acrylic acid hydrogel synthesized via electron beam irradiation: Accelerated burn wound healing in an animal model. *J Carbohydrate Polymers,* 114**,** 312-320.

Moreno, E., Schwartz, J., Larrea, E., *et al.* 2015. Assessment of β-lapachone loaded in lecithin-chitosan nanoparticles for the topical treatment of cutaneous leishmaniasis in L. major infected BALB/c mice. *J Nanomedicine: Nanotechnology, Biology Medicine,* 11**,** 2003-2012.

Na, R. & Wei, T. 2021. Recent perspectives of nanotechnology in burn wounds management: a review. *J Journal of Wound Care,* 30**,** 350-370.

Norouzi, M., Boroujeni, S. M., Omidvarkordshouli, N., *et al.* 2015. Advances in skin regeneration: application of electrospun scaffolds. *J Advanced healthcare materials,* 4**,** 1114-1133.

O'neill, A. J. & Chopra, I. 2004. Preclinical evaluation of novel antibacterial agents by microbiological and molecular techniques. *J Expert opinion on investigational drugs,* 13**,** 1045-1063.

Osuka, A., Ogura, H., Ueyama, M., *et al.* 2014. Immune response to traumatic injury: harmony and discordance of immune system homeostasis. *J Acute Medicine,* 1**,** 63-69.

Parveen, R., Baboota, S., Ali, J., *et al.* 2011. Oil based nanocarrier for improved oral delivery of silymarin: in vitro and in vivo studies. *J International journal of pharmaceutics,* 413**,** 245-253.

Pourali, P., Razavianzadeh, N., Khojasteh, L., *et al.* 2018. Assessment of the cutaneous wound healing efficiency of acidic, neutral and alkaline bacterial cellulose membrane in rat. *J Journal of Materials Science: Materials in Medicine,* 29**,** 1-9.

Rae, L., Fidler, P. & Gibran, N. 2016. The physiologic basis of burn shock and the need for aggressive fluid resuscitation. *J Critical care clinics,* 32**,** 491-505.

Rai, M., Yadav, A. & Gade, A. 2009. Silver nanoparticles as a new generation of antimicrobials. *J Biotechnology advances,* 27**,** 76-83.

Rech, M. A., Mosier, M. J., Mcconkey, K., *et al.* 2019. Outcomes in burn-injured patients who develop sepsis. *J Journal of Burn Care Research,* 40**,** 269-273.

Rigo, C., Ferroni, L., Tocco, I., *et al.* 2013. Active silver nanoparticles for wound healing. *J International journal of molecular sciences,* 14**,** 4817-4840.

Rowan, M. P., Cancio, L. C., Elster, E. A., *et al.* 2015. Burn wound healing and treatment: review and advancements. *J Critical care,* 19**,** 1-12.

Rubenick, J. B., Rubim, A. M., Bellé, F., *et al.* 2017. Preparation of mupirocin-loaded polymeric nanocapsules using essential oil of rosemary. *J Brazilian Journal of Pharmaceutical Sciences,* 53**,** e16101.

Sanad, R. A., Abdelmalak, N. S., Elbayoomy, T. S., *et al.* 2010. Formulation of a novel oxybenzone-loaded nanostructured lipid carriers (NLCs). *J Aaps Pharmscitech,* 11**,** 1684-1694.

Schneider, L. A., Korber, A., Grabbe, S., *et al.* 2007. Influence of pH on wound-healing: a new perspective for wound-therapy? *J Archives of dermatological research,* 298**,** 413-420.

Sidossis, L. S., Porter, C., Saraf, M. K., *et al.* 2015. Browning of subcutaneous white adipose tissue in humans after severe adrenergic stress. *J Cell metabolism,* 22**,** 219-227.

Singh, R. & Lillard Jr, J. W. 2009. Nanoparticle-based targeted drug delivery. *J Experimental molecular pathology,* 86**,** 215-223.

Spelman, D. 1999. Fusidic acid in skin and soft tissue infections. *J International journal of antimicrobial agents,* 12**,** S59-S66.

Vashishth, V. & Kaushik, D. 2017. Mupirocin amalgamated inorganic nanoparticles for augmenting drug delivery in resistant microbial strains. *J World J Pharm Pharm Sci***,** 1214-29.

Wiley, B., Sun, Y., Mayers, B., *et al.* 2005. Shape-controlled synthesis of metal nanostructures: the case of silver. *J Chemistry–A European Journal,* 11**,** 454-463.

Williamson, D. A., Carter, G. P. & Howden, B. P. 2017. Current and emerging topical antibacterials and antiseptics: agents, action, and resistance patterns. *J Clinical microbiology reviews,* 30**,** 827-860.

Wolfe, C. R. 2011. Case report: treatment of chronic osteomyelitis. *J Clinical infectious diseases,* 52**,** S538-S541.

Xie, Z., Paras, C. B., Weng, H., *et al.* 2013. Dual growth factor releasing multi-functional nanofibers for wound healing. *J Acta biomaterialia,* 9**,** 9351-9359.

Zahedi, P., Rezaeian, I., Ranaei-Siadat, S. O., *et al.* 2010. A review on wound dressings with an emphasis on electrospun nanofibrous polymeric bandages. *J Polymers for Advanced Technologies,* 21**,** 77-95.

Zhang, L., Pornpattananangkul, D., Hu, C.-M., *et al.* 2010. Development of nanoparticles for antimicrobial drug delivery. *J Current medicinal chemistry,* 17**,** 585-594.

Zhu, X., Radovic-Moreno, A. F., Wu, J., *et al.* 2014. Nanomedicine in the management of microbial infection–overview and perspectives. *J Nano today,* 9**,** 478-498.